

Groove-Induced Drag Reduction in Annular Flows

H. V. Moradi and J.M. Floryan

Department of Mechanical and Materials Engineering
 The University of Western Ontario, London, Ontario, N6A5B9, Canada

Abstract

Laminar pressure driven flows through annuli fitted with longitudinal grooves with an arbitrary cross-section have been analyzed. It is demonstrated that a reduced order model is an effective tool for extraction of geometric features that lead to the drag generation. It is shown that presence of the grooves may lead to a reduction of pressure loss in spite of increase of the surface wetted area. The drag decreasing grooves are characterized by the groove wave number M/R_1 being smaller than a certain critical value, where M denotes the number of grooves being used and R_1 stands for the radius of the annulus. It is shown that the drag reduction mechanism relies on the re-arrangement of the bulk flow which leads to the largest mass flow taking place in the area of the largest annulus opening. Form of the optimal grooves, from the point of view of the maximum drag reduction, has been determined.

Introduction

Reduction of pressure losses associated with movement of fluids through conduits attracted special attention in recent times due to an increase in the cost of energy and an interest in the reduction of environmental impact. Most of the fundamental work has been devoted to the classical canonical flows, e.g., pressure driven flow either through a plane channel or through a circular pipe, kinematically driven flows (Couette flow), and various forms of boundary layers (the Blasius and the Falkner-Skan boundary layers). This work focuses on another, less studied but nevertheless technologically important flow, i.e. a pressure driven flow through an annulus formed by two concentric cylinders. This flow is encountered in petroleum engineering, heat exchangers, turbomachinery, fuels cells, aero-engines and various chemical industrial devices, and its character has a significant impact on the efficiency of these devices. The question of stability of the annular flow and an understanding of the transition between the laminar and turbulent states represents a classical problem that has been studied for over fifty years. Heaton [8] provides a summary of the current results in this area. The available transition prediction criteria are discussed in [4]. A number of important variations of this flow have also been studied. Spiral flow occurs when one of the cylinders is subject to a rotation; a review of the relevant literature can be found in [3]. Recent results on the effects of eccentricity in the location of the cylinders are discussed in [16]. Progress in modeling of the effects of surface roughness is well summarized in [13].

Variations in the structure of surface topography offers potential for improving the performance of flow systems, following examples found in biology [10]. Shark skin represents a good example of a low drag surface. The skin is covered with very small, tooth-like scales ribbed with longitudinal grooves which reduce the formation of vortices present on a smooth surface. The leaves of the lotus plant provide an example of a super-

hydrophobic and a low drag surface. The special properties of this surface are associated with wax tubules that create a certain surface topography. Surface topography affects the form of turbulence [9], plays a large role in the laminar-turbulent transition [5], and is used as a mixing augmentation technique in heat transfer [13]. The above examples illustrate the potential gains associated with the use of the properly selected surface structures, but one needs to achieve a complete understanding of the processes induced by these structures in order to take the full advantage of this potential.

One particular form of surface topography, i.e. longitudinal grooves/ribs, commonly referred as riblets, have attracted attention due to their drag reducing capabilities in turbulent flow regimes [15,16]. Such grooves have a wavelength of the order of the viscous scale and reduce the shear drag through an interference with the turbulence production. The viscous regime of vanishing riblet spacing is well understood [1,11]. Results of detailed measurements of the drag reduction for various riblet shapes have been summarized in [2,6]. For larger riblets, the minimum drag is related to the breakdown of the viscous regime and this process is less understood [7]. Laminar riblets attracted less attention. Mohammadi & Floryan [12] considered pressure-driven laminar flows and demonstrated drag reducing abilities of long wavelength grooves associated with the redistribution of the bulk flow.

This work is focused on the analysis of laminar, pressure driven flows in annuli outfitted with longitudinal grooves of arbitrary shape and on the systematic search for the forms of such grooves that are able to reduce drag. The drag-reducing abilities are assessed by determining the additional pressure gradient required to maintain the same mass flow rate through the groove-fitted as well as through the smooth annuli.

Problem formulation

Consider steady axial flow in an annulus bounded by two coaxial cylinders fitted with longitudinal grooves, as illustrated in Fig.1. There are M identical grooves of an arbitrary shape over the circumference and thus wall geometries can be expressed as

$$r_{in}(\theta) = R_1 + \sum_{n=-N_A}^{N_A} H_{in}^{(n)} e^{inM\theta}, r_{out}(\theta) = 1 + R_1 + \sum_{n=-N_A}^{N_A} H_{out}^{(n)} e^{inM\theta} \quad (2.1)$$

where R_1 and $1 + R_1$ are the radii of the smooth reference inner and outer cylinders, $H_{in}^{(n)} = H_{in}^{(-n)*}$, $H_{out}^{(n)} = H_{out}^{(-n)*}$ are the reality conditions, stars denote the complex conjugates, N_A is the number of Fourier modes required for description of the shape of

the grooves, and all quantities have been scaled with the gap L between the reference cylinders as the length scale.

The flow is driven by a constant axial pressure gradient which leads to a velocity field with the velocity vector having components $(v, 0, 0)$ in the (z, r, θ) directions. This field is completely described by the axial momentum equation in the form

$$\left(\frac{1}{r} \frac{\partial v}{\partial r} + \frac{\partial^2 v}{\partial r^2} + \frac{1}{r^2} \frac{\partial^2 v}{\partial \theta^2} \right) = Re \frac{\partial p}{\partial z}$$

which has been scaled using the maximum of the axial velocity of the reference flow U_{max} as the velocity scale and ρU_{max}^2 as the pressure scale where ρ stands for the density. The Reynolds number is defined as $Re = U_{max} L / \nu$ where ν stands for the kinematic viscosity. The boundary conditions have the form

$$v(r, \theta) = 0 \text{ at } r = r_{in}(\theta) \text{ and } r = r_{out}(\theta).$$

The problem of determination of the effects of the grooves is posed as the problem of determination of an additional pressure gradient required in order to maintain the same flow rate in the grooved annulus as in the reference smooth annulus. This necessitates introduction of the flow rate constraint in the form

$$Q = M \int_0^{2\pi/M} \int_{r_{in}(\theta)}^{r_{out}(\theta)} r v dr d\theta$$

where Q is the known flow rate; this flow rate is equal to the flow rate in the corresponding smooth annulus.

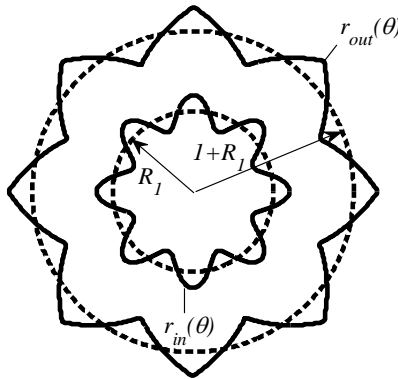


Figure 1. Sketch of the flow geometry - annulus with longitudinal grooves with an arbitrary geometry.

The reference flow, i.e. flow in a smooth annulus, has the velocity distribution, the pressure gradient and the flow rate expressed as

$$v_0(r) = R_1^2 [1 - (r/R_1)^2] / k_1 + k_2 \ln(r/R_1) / k_1,$$

$$dp_0/dz = -4/k_1 Re$$

$$Q_0 = 2\pi \left[\frac{(1 + R_1)^2 (R_1^2 - 2R_1 - 1 - k_2) / 4 + k_2 (1 + R_1)^2 \ln((1 + R_1)/R_1) / 2 + R_1^2 (k_2 - 1) / 4}{k_1} \right]$$

where $k_1 = R_1^2 - k_2 \ln R_1 + k_2 / 2 [\ln(k_2/2) - 1]$ and $k_2 = (1 + 2R_1) / \ln[(1 + R_1)/R_1]$. The maximum of v_0 occurs at $r = \sqrt{k_2/2}$ and this defines the velocity scale U_{max} .

The problem is solved by analytically mapping the irregular flow domain onto a rectangular strip in the (r, θ) plane, discretizing the

resulting equations using Fourier expansions in the θ -direction and Chebyshev expansions in the r -direction, and using Galerkin projection method to convert the differential system into an algebraic system. This procedure provides spectral accuracy.

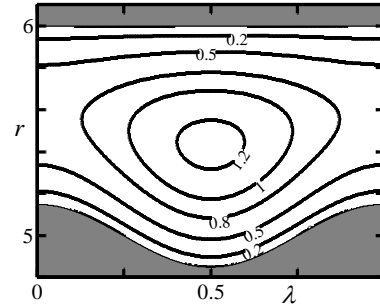


Figure 2. Distribution of the axial velocity component in an annulus with the inner cylinder with the average radius $R_1=5$ fitted with five sinusoidal grooves with the amplitude $S_m=0.3$ and a smooth outer cylinder.

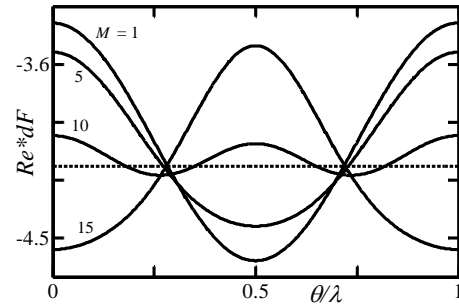


Figure 3. Distribution of the axial component of shear stress acting on the fluid at the inner cylinder for the same geometry as in Fig.2 but with the inner cylinder fitted with $M = 1, 5, 10, 15$ grooves. Dashed line provides reference value for the smooth cylinders.

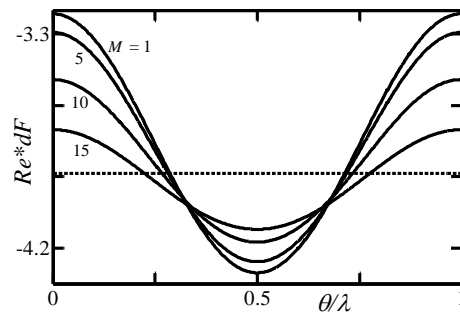


Figure 4. Distribution of the axial component of shear stress acting on the fluid at the outer cylinder. Other conditions as in Fig.3.

Results

There is an uncountable number of possible groove shapes and positions. It can be shown [12] that the complete effect can be decomposed into (i) an effect due to the change in the average position of each cylinder (i.e. change of the flow cross-sectional area) and (ii) an effect due to the spatial flow modulations created by the grooves. The former one can be accounted for analytically and, thus, this presentation is focused on the modulation effect.

The reduced order model based on the use of the leading Fourier mode from the Fourier expansion describing geometry of the wall permits determination of changes of the friction factor with accuracy of at least 10% in the case of channel flows [12]. The same model is used in the present analysis.

Figure 2 displays velocity contours for an annulus with the drag reducing grooves. It can be seen that the mass flow rate concentrates in the area of the largest annulus opening. Figure 3 displays distribution of shear stress at the grooved wall for the annulus fitted with different numbers of grooves. A qualitative change in the distribution of the shear associated with the change from the drag reducing to the drag increasing system (when M increases above the critical value) can be observed. Figure 4 displays shear stress at the outer smooth wall under the same conditions. It can be seen that the grooves have a marginal effect on this shear. Figure 5 displays variations of the modification friction factor normalized with the friction factor for the smooth cylinder with either the inner or the outer cylinder fitted with the grooves. It can be seen that the radius of the inner cylinder has to be sufficiently large to produce drag reduction, the magnitude of the reduction increases with the amplitude of the grooves, and grooves placed at the inner cylinder are more effective than the same grooves placed at the outer cylinder.

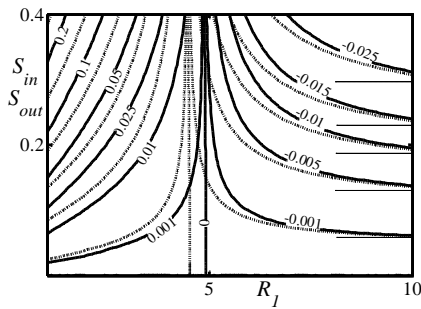


Figure 5. Variations of the modification friction factor normalized with the friction factor for the smooth annulus as a function of the groove amplitudes S_{in} (inner cylinder) and S_{out} (outer cylinder) and the radius of the inner cylinder R_1 for the groove geometry described by one Fourier mode for $M = 15$ grooves. Solid (dash) lines correspond to grooves placed only at the inner (outer) cylinder.

The above results have been obtained for grooves with shape represented by a single Fourier mode. Determination of the most effective shape requires use of optimization procedure with constraints guaranteeing preservations of the same annulus cross-sectional area and preventing contact between both cylinders. It was assumed in the analysis that the number of grooves M , the cylinder radius R_1 , and the maximum permitted height and the maximum permitted depth of the grooves were specified and kept constant during optimization. Groove shape was represented by a Fourier expansion and the optimization process identified coefficients of such expansion. It has been found that these expansions converged rapidly and 4-5 Fourier modes were sufficient to describe the optimal shape.

Figure 6 shows that the optimal shape in the case of grooves with the same height and depth can be well approximated by a trapezoid. Figure 7 illustrates changes in the friction factor resulting from the use of such grooves. It can be seen that these grooves provide up to 25% better performance. Their advantage increases with an increase of the groove amplitude.

The same optimization process carried out with a fixed height of the grooves but with their depth being one of the variables results in grooves that can be well approximated using a delta function, as shown in Fig.8.

Conclusions

An analysis of the laminar flows through annuli fitted with longitudinal grooves has been carried out. Forms of the grooves that result in the reduction of the pressure gradient below the

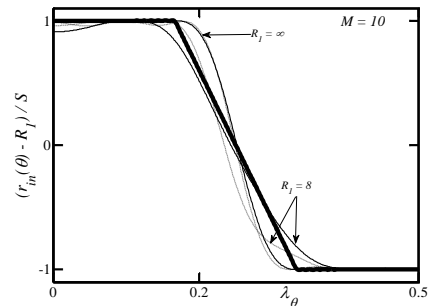


Figure 6. Evolution of the optimal shape of $M = 10$ equal-depth grooves placed at the inner cylinder as a function of the wall curvature R_1 . Solid, dashed and dotted lines correspond to the depth of the grooves $S_{in,i} = S_{in,o} = S = 0.2, 0.5, 0.8$, respectively. Thick lines describe the universal shape, i.e. trapezoid with $a = b = \lambda/6$ and $c = d = \lambda/3$.

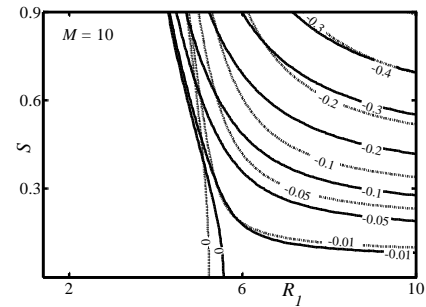


Figure 7. Variations of the modification friction factor normalized with the smooth annulus friction factor as a function of the cylinder curvature R_1 and the groove amplitude S for $M = 10$ equal-depth trapezoidal grooves placed at the inner cylinder. Dashed lines are for the sinusoidal grooves with the same amplitude.

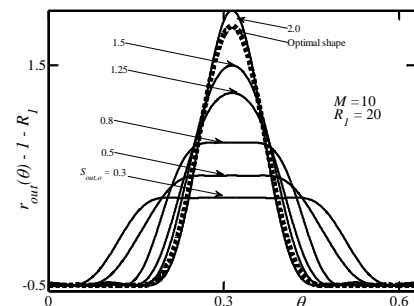


Figure 8. Evolution of the optimal shape of the unequal-depth grooves placed at the outer cylinder as a function of the depth of the groove $S_{out,o}$. The height of the groove is set at $S_{out,i} = 0.5$, $M = 10$ grooves are used

and the cylinder radius of curvature is $R_1 = 20$. Dashed lines illustrate shapes corresponding to the optimal depth.

level needed to maintain the same flow rate as in a smooth annuli have been identified. A reduced order model has been used as a tool for the extraction of features of groove geometry that lead to drag reduction. It is shown that the presence of the grooves may lead to a reduction of pressure loss in spite of an increase of the surface wetted area. The drag decreasing grooves are characterized by the groove wave number M/R_1 being smaller than a certain critical value, where M denotes the number of grooves being used and R_1 stands for the radius of the annulus. It is shown that the drag reduction mechanism relies on the re-arrangement of the bulk flow that leads to the largest mass flow taking place in the area of the largest annulus opening. A search for the form of the grooves that results in the largest decrease of the drag, i.e. the optimal shape, has been carried out. It has been found that in the case of the equal-depth grooves the optimal shape changes very little as a function of the flow and geometry parameters and can be approximated using a special form of trapezoid. Drag reduction is a non-monotonic function of groove's depth in the case of the unequal-depth grooves. The depth that gives the largest drag reduction for a given height, the optimal depth, as well as the corresponding groove shape define the optimal geometry. Properties of the optimal geometry can be determined directly through the optimization process. It is shown that the optimal shape forming the optimal geometry can be approximated using a delta function.

Acknowledgments

This work has been carried out with the support of NSERC of Canada.

References

- [1] Bechert, D.W., Bartenwerfer, M., The viscous flow on surfaces with longitudinal ribs, *J. Fluid Mech.*, 206, 1989, 105–129.
- [2] Bechert, D.W., Bruse, M., Hage, W., Van Der Hoeven, J.G.T., Hoppe, G., Experiments on drag-reducing surfaces and their optimization with an adjustable geometry, *J. Fluid Mech.*, 338, 1997, 59–87.
- [3] Cotrell, D.L., Pearlstein, A.L., Linear stability of spiral and annular Poiseuille flow for small radius ratio, *J. Fluid Mech.*, 547, 2006, 1-20.
- [4] Dou, H.S., Khoo, B.C., & Tsai, H.M., Determining the critical conditions of turbulent transition in a fully developed annulus flow, *J. Petroleum Science and Engineering*, 73, 2010, 41-47.
- [5] Floryan, J. M., Three-dimensional instabilities of laminar flow in a rough channel and the concept of hydraulically smooth wall, *Eur. J. Mech. B/Fluids*, 26, 2007, 305–329.
- [6] Frohnäpfel, B., Jovanović, J., Delgado, A., Experimental investigations of turbulent drag reduction by surface-embedded grooves, *J. Fluid Mech.*, 590, 2007, 107–116.
- [7] Garcia-Mayoral, R., & Jimenez, J., Hydrodynamic stability and breakdown of the viscous regime over riblets, *J. Fluid Mech.*, 678, 2011, 317-347.
- [8] Heaton, C.J., Linear instability of annular Poiseuille flow, *J. Fluid Mech.*, 610, 2008, 391-406.
- [9] Jimenez, J., Turbulent flows over rough walls, *Ann. Rev. Fluid Mech.*, 36, 2004, 173–196.
- [10] Jung, Y.C., Bhushan, B., Biomimetic structures for fluid drag reduction in laminar and turbulent flows, *J. Phys.: Condens. Matter*, 22, 2010, 035104, 1–9.
- [11] Lucini, P., Manzo, F., Pozzi, A., Resistance of grooved surface to parallel flow and cross-flow, *J. Fluid Mech.*, 228, 1991, 87-109.
- [12] Mohammadi, A., Floryan, J.M., Pressure Losses in Grooved Channels, Expert Systems in Fluid Dynamics Research Laboratory Report ESFD-4/2011, Department of Mechanical and Materials Engineering, The University of Western Ontario, London, Ontario, N6A 5B9, Canada, 2011.
- [13] Valdes, J.R., Miana, M.J., Pelegay, J.L., Nunez, J.L., Pütz, T., Numerical investigation of the influence of roughness on the laminar incompressible fluid flow through annular microchannels, *Int. J. Heat Mass Transfer*, 50, 2007, 1865-1878.
- [14] Walsh, M. J., Drag characteristics of V-groove and transverse curvature riblets. In *Viscous Drag Reduction* (ed. G. R. Hough), AIAA, 72, 1980, 168–184.
- [15] Walsh, M. J., Riblets as a viscous drag reduction technique, *AIAA J.*, 21, 1983, 485–486.
- [16] Walton, A.G., Labadin, J., Yiong, S.P., Axial flow between sliding, non-concentric cylinders with applications to thread injection, *Quarterly Journal of Mechanics and Appl. Math.*, 63, 2010, 315-334.